BEAM HALO OBSERVATION BY CORONAGRAPH

T. Mitsuhashi, KEK, TSUKUBA, Japan

Abstract

We have developed a coronagraph for the observation of the beam halo surrounding a beam. An opaque disk is set in the beam image plane to block the glare of the beam image. We succeeded in obtaining a signal to background ratio of $6x10^{-7}$. As a test, we tried to observe the beam halo at the Photon Factory storage ring. We succeeded in observing the tail of the beam, which has an intensity range of 10^{-4} to 10^{-6} of the peak intensity.

INTRODUCTION

The beam tail or halo is one of the significant problems in proton machines and future Linac-based machines such as LC and ERL. To develop an apparatus to observe the beam tail or halo, we used the concept of the coronagraph. The coronagraph is a spatial telescope observing the sun-corona via artificial eclipse [1]. The concept of this apparatus is to create an artificial eclipse by blocking the glare of the sun's image and thereby observe the weak image of the sun's corona. We applied this concept to the observation of the halo surrounding a beam. In the coronagraph, the diffraction fringe surrounding the sun image is eliminated by a re-diffraction system with a mask (Lyot stop). Since the background mainly comes from scattered light from defects in the objective lens, such as scratches and digs on the surface, the key point to realize good performance of the coronagraph is to reduce scattering light from the objective lens. We used a very well-polished lens for the objective lens, and succeeded in obtaining a signal to background ratio of better than 10^{-6}. We observed the beam halol by coronagraph at the Photon Factory storage ring. We succeeded in observing the halo of the beam which has an intensity range from $1/10^4$ to $1/10^6$ of the peak intensity. The use of the words beam halo or beam tail can introduce some confusion: I use the word "halo" to mean both beam halo and beam tail in this paper.

BEAM HALO OBSERVATION WITH NORMAL TELESCOPE

Let us consider the observation of the sun's corona with a normal telescope. To create an artificial eclipse, we can set an opaque disk on the focal plane of the objective lens to block the glare of the sun image as shown in Fig. 1. In the normal telescope setup, the objective lens aperture makes a bright diffraction fringe surrounding from the sun image. The ratio of intensities between the diffraction fringes to the peak of the Airy disc is approximately 10^{-2} at the first peak of the fringe. These intense diffraction fringes inhibit the observation of the weak image of the sun corona which has an intensity range of 10^{-5}.

In the case of beam halo observation with typical beam profile monitor using the visible synchrotron radiation in the particle accelerator, we have the same difficulty as in the sun corona observation. Let us consider the observation of beam halo at the Photon Factory. As shown in Fig.2, the second diffraction fringe has the same intensity as the geometrical image of the beam. The beam halo near the third diffraction fringe has a weaker intensity than the diffraction fringe, and we cannot observe it by a normal imaging method as in the SR profile monitor.

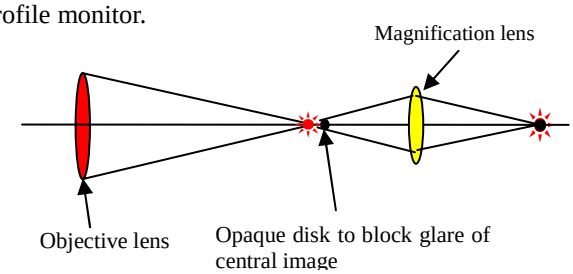

Figure 1: Set up of normal telescope with opaque disk.

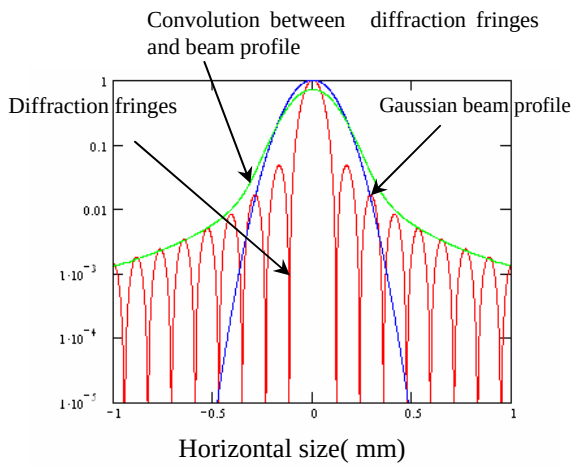

Figure 2: Comparison of the beam profile and point spread function (PSF). The solid red line denotes the PSF, and the blue line denotes the Gaussian horizontal beam profile at the Photon Factory.

CONCEPT OF THE CORONAGRAPH

The optical layout of the coronagraph is illustrated in Fig.3. The first lens (objective lens) makes a real image of the object (beam image) on to a blocking opaque disk which creates an artificial eclipse. A second lens (field lens) is set just after the blocking disk. The focusing length of the field lens is chosen to make a real image of the objective lens aperture onto a mask (Lyot Stop). The diffraction fringe in the focal plane of the objective lens is not blocked by the opaque disk, and is re-diffracted by the field lens aperture. Then the re-diffracted light makes another diffraction fringe around the geometrical image of

the objective lens aperture in the focal plane of the field lens. Lyot's brilliant idea for the coronagraph is to remove this diffraction fringe by a mask, and relay the hidden weak image by a third lens onto the final observation plane [1]. The background light on the final observation plane now mainly come from the scattering of the input light by the objective lens. By utilizing a very well polished lens as the objective, we can reduce the background light to less than 10^{-6} of the main image.

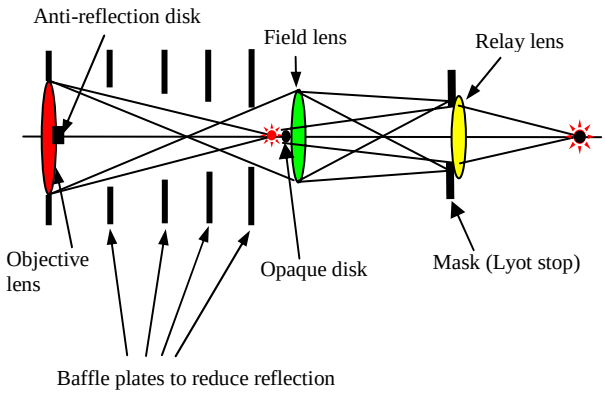

Figure 3: Layout of optical system of the coronagraph.

FUNCTION OF RE-DIFFRACTION SYSTEM TO ELIMINATE DIFFRACTION FRINGE

To eliminate the intense diffraction fringes, a re-diffraction optics system is used in the coronagraph. In the optical system of the coronagraph, the disturbance of the light to the field lens aperture is diffracted again, and produces re-diffraction fringes onto its focal plane. By this reason, the second field lens in the system is called the re-diffraction system. The function of the re-diffraction system in eliminating diffraction fringes in the coronagraph is illustrated in Fig 4. As illustrated in Fig. 4 (a), the aperture of the objective lens makes diffraction fringes in its focal plan. The glare of the central image is blocked by the opaque disk as illustrated in Fig. 4 (b). The entrance pupil of the next field lens is the aperture of the lens pupil with a stop, with the diameter of the opaque disk. Then the input disturbance of the light is diffracted again with this aperture, making diffraction fringes on the focal plane of the field lens. Letting F(ξ) denote the disturbance of the light on the imaging plane of the objective lens, the disturbance of the re-diffracted light u(x) on the imaging plane of the field lens is given by,

$$u(x) = \frac{1}{i \cdot \lambda \cdot f} \int_{\xi 1}^{\xi 2} F(\xi) \exp\left\{ - \frac{i \cdot 2 \cdot \pi \cdot x \cdot \xi}{\lambda \cdot f} \right\} d\xi \ ,$$

where λ denotes the wavelength of the input light, $\xi 1$ denotes the radius of the stop, $\xi 2$ denotes the radius of the aperture at the pupil of the field lens, and f denotes the distance between the field lens and its imaging plane. An example of the simulation of the intensity distribution $u^2(x)$ using an input square aperture at the objective lens is shown in Fig. 5. From this figure, we can see two diffraction sets of rings located in the inside and outside of the geometrical image of objective lens edge. As illustrated in Fig.4 (c), by hiding this diffraction ring with a mask (Lyot Stop), the light from the diffraction fringe will not come to the later stage of the coronagraph.

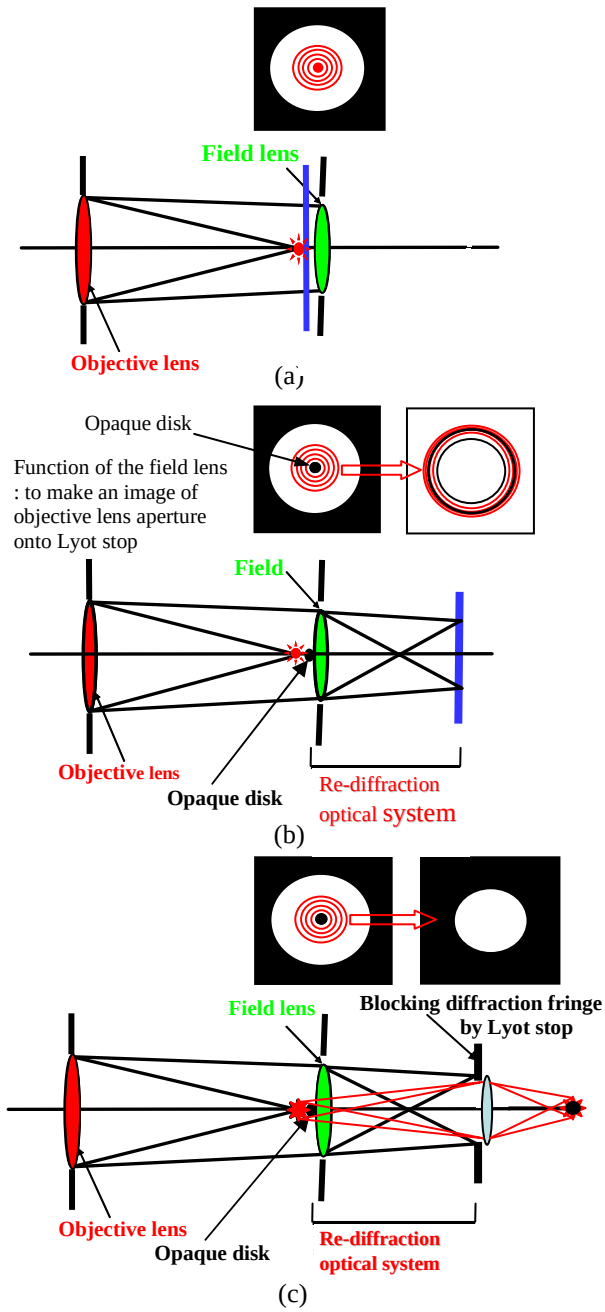

Figure 4: Function of re-diffraction system to eliminate diffraction fringes in the coronagraph. (a) Diffraction by objective lens. (b) The field lens makes an image of the objective lens aperture onto the Lyot stop. Re-diffraction fringes appear inside and outside of the geometrical image of the objective lens aperture. (c) Re-diffraction fringes are blocked by the Lyot stop. The surrounding weak image will be relayed to the final focusing point.

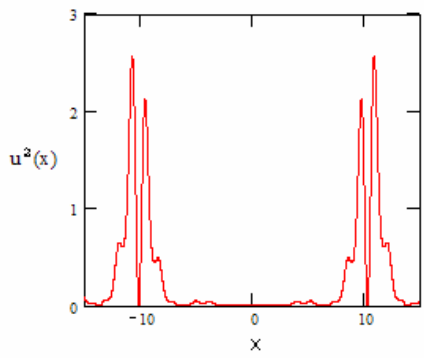

Figure 5: A simulation of the intensity distribution $u^2(x)$ using a square input aperture on the objective lens. The valley between the diffraction peaks corresponds to the position of the geometrical image of the aperture edge of the objective lens.

BACKGROUND FROM THE OBJECTIVE LENS

The glare of the central image is blocked by the opaque disk, and the diffraction fringes are eliminated by the re-diffraction system with the Lyot stop. The remaining measured background is scattered light from the defects in the objective lens such as scratches and digs on its surfaces. This scattered light intensity can reach 0.1% of the input light intensity. To eliminate this scattering background, we must polish the lens carefully to remove such scratches and digs on the lens surfaces. Figure 6 shows a microscope image of a well-polished surface for the object lens compared with a typical surface with optical polishing to scratch & dig 60/40. In these figures, surfaces are illuminated from the side (dark field illumination method). The surface of the lens with optical polishing to scratch & dig 60/40 still has many digs (small spots in the photograph). The surface of the objective lens using careful polishing has almost no digs.

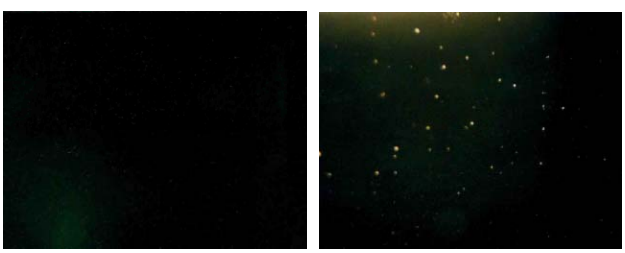

(a) (b)

Figure 6: Microscope image of the digs on the surface of lens illuminated from the side. (a) Surface of objective lens for coronagraph. (b) Surface with optical polishing to scratch & dig 60/40. The side of this picture is 5mm.

OBSERVATON OF BEAM HALO AT THE PHOTON FACTORY

To investigate the performance of the coronagraph, we observed the beam halo at the Photon Factory.

Design of Coronagraph

A well-polished singlet lens made of BK7 having a diameter of 150 mm is used as an objective lens. To reduce spherical aberration, the shape of the lens is chosen to be concave-flat. The focal length of the objective lens is chosen to be 2000 mm to obtain a sufficient size of the beam image on the blocking disc. A square aperture is set just in front of the objective lens to define the entrance pupil. We prepared cone-shaped opaque disks as shown in Fig. 6. The opaque disk is set on a 3-d movable stage for the adjustment of the transverse and longitudinal positions of the disk relative to the beam image. The opaque disk assembly is set in front of the field lens to block the glare of the central beam image. The diameter of the opaque disk is chosen to block 4 σ of the beam size.

Figure 7: Photograph of the opaque disk to block the glare of central image.

An ED achromatic lens having a focal length of 500 mm with a diameter of 50 mm is used as the field lens. A quadratic slit is set in the imaging plane of the field lens as the Lyot stop. A band-pass filter of 550 nm with a bandwidth of 10 nm and dichroic polarization filter are set before the Lyot stop. We used two ED achromatic lenses for the final image relay system. A high-speed gated camera (Hamamatsu photonics C2925-01) is used for the observation of the final image.

Low-noise mirror for the light transport line

The SR monitor has a light transport line between the source point and the observation system such as the coronagraph. The visible SR is extracted by a water-cooled mirror made of beryllium. Then the visible SR is relayed to the dark room by three mirrors made of fused silica. The surface scattering of the Be mirror is rather large due to many digs on the surface. But this Be mirror is located near the source point, and far from the coronagraph. The estimated contribution of background noise from the Be-mirror is about 5×10^{-7} due to the distance between the mirror and the coronagraph. We have a final mirror in the light transfer line in 2 m front of the coronagraph, and the contribution to the background from this mirror is estimated to be 6×10^{-5}. This background is too strong for beam halo observation. We replaced this mirror with a newly made low-noise mirror. As a low noise mirror, we used a well-polished optical flat of the same quality as that of the objective lens of the

coronagraph having a backside Al coating as shown in Fig. 8. To eliminate a ghost image from surface reflection, we applied a small wedge angle (10 arcsec) between both surfaces as shown in Fig. 8. Since the arrangement of back side coating and quasi-parallel surfaces will easily produce interference fringes, this small wedge angle is also important to eliminate the contrast of interference fringes in the ray.

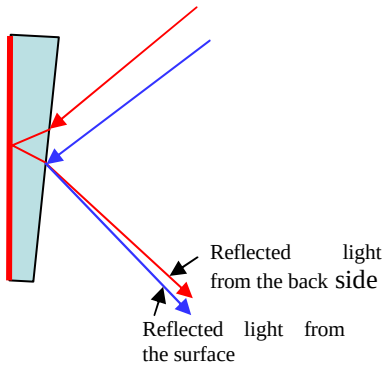

Figure 8: Low-noise mirror for light transport line.

Observation of beam halo

At first, we observed an image of the stored beam profile without the opaque disk and Lyot stop. The result is shown in Fig. 9.

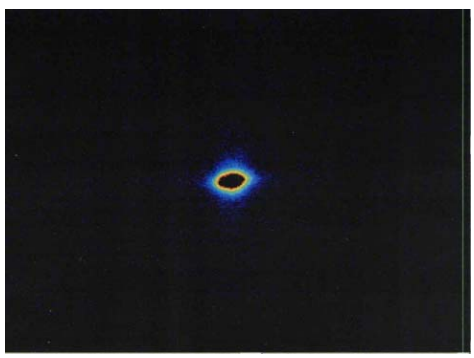

Figure 9: Image beam profile without the opaque disk. Exposure time of CCD camera is 10μsec.

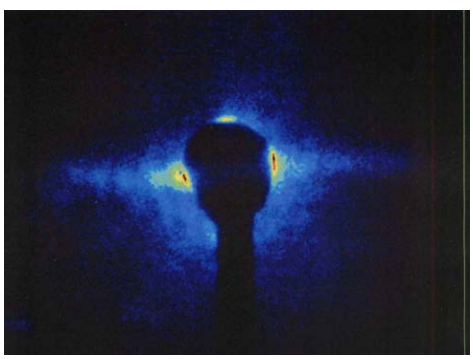

Figure 10: Image of beam halo with the opaque disk. Transverse magnification is same as in Fig. 9. Exposure time of CCD camera is 10 msec.

The exposure time to catch this image was 10 μsec. Next, we observed an image of the beam halo by applying the opaque disk to blocking the central beam image and Lyot stop. Since the intensity of the beam halo image is very weak, we increased the exposure time of the CCD camera. An example of the beam halo image is shown in Fig. 10. The exposure time was 10 msec. Considering the differences in exposure time, the intensity scale in Fig.10 is 1000 times smaller than the intensity scale in Fig 9.

Observation of beam halo with diffraction

On trial, to investigate the effect of diffraction in the halo observation, we observed an image with opaque disk and without Lyot stop. An example is shown in Fig.11. In this figure, we rotate the square entrance pupil by 30 deg for the easy discrimination of the diffraction effect. We can see the tilted diffraction halo in this figure.

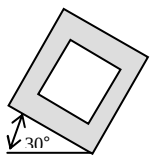

Entrance pupil is intentionally rotated by 30° to recognize diffraction tail easily.

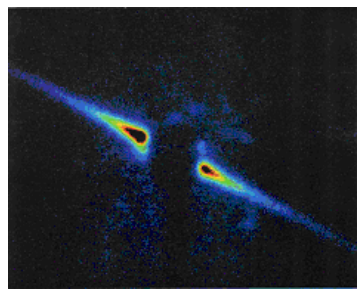

Figure 11: Halo with diffraction observed with opaque disk and without Lyot stop.

A comparison of intensities of halos measured with and without opaque disk and Lyot stop are shown in Fig.12. Both intensities are normalized by the peak intensity of the central beam image. As discussed in Section 1, the beam halo image with diffraction observed without Lyot stop has an intensity range of 10^{-2} of the peak.

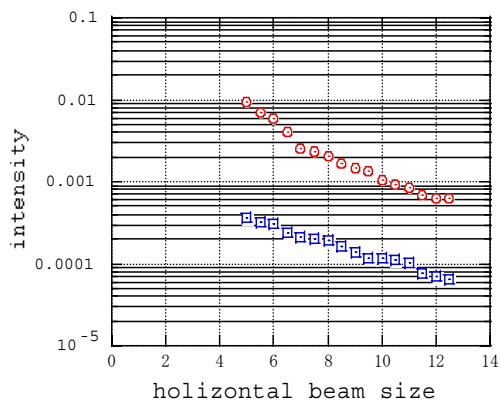

Figure 12: Comparison of beam tails; circles denote beam halo without opaque disk. The red circles denote halo with diffraction. The blue squares denote beam halo measured with opaque disk and Lyot stop. The horizontal axis is normalized by 1σ of the beam size.

Observation of beam halo at different ring currents

The beam halo images are observed at several ring currents in the single bunch operation of the Photon Factory. Results are shown in Fig. 13. For an example at small beam current, the beam tail image which is observed in the multi-bunch operation is also shown in Fig. 13. The corresponding bunch current is 1.4 mA. The intensity of the beam halo becomes stronger as the bunch current is increased. Not only the intensity, but also the two-dimensional distributions of the beam halo are changed in this figure. Particularly in the vertical axis, the area of the beam halo is enlarged as the beam current increases.

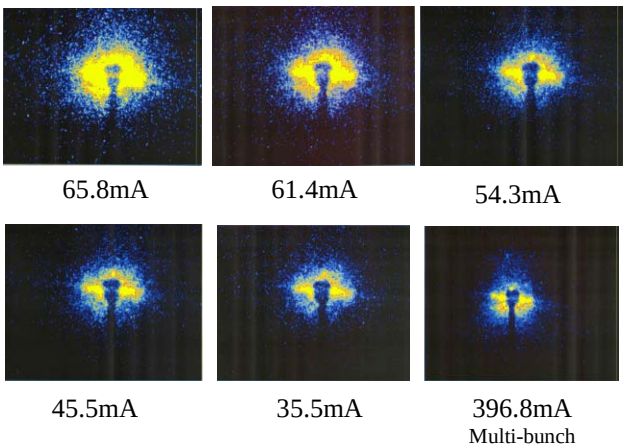

Figure 13: Beam halo observed at different ring currents in the Photon Factory.

Observation of far outside beam halo

As seen in Fig.13, the area occupied by the beam halo does not increase in the horizontal direction as the beam current increases. To investigate the beam halo far outside in the horizontal, we block the strong halo area. This time, an opaque stick was used instead of the opaque disk. An example is shown in the lower picture of Fig.14.

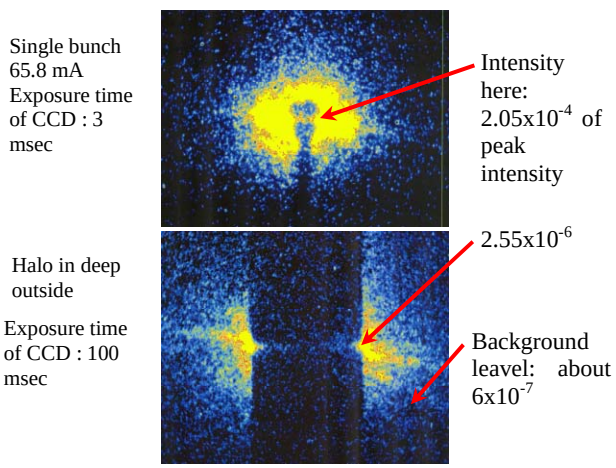

Figure 14: Observation of far outside halo at the Photon Factory.

The exposure time for this observation was increased to 100 msec. This exposure time is about 33 times longer than that in Fig.13. The projection of the horizontal distributions of the beam halos in Fig.14 is shown in Fig. 15.

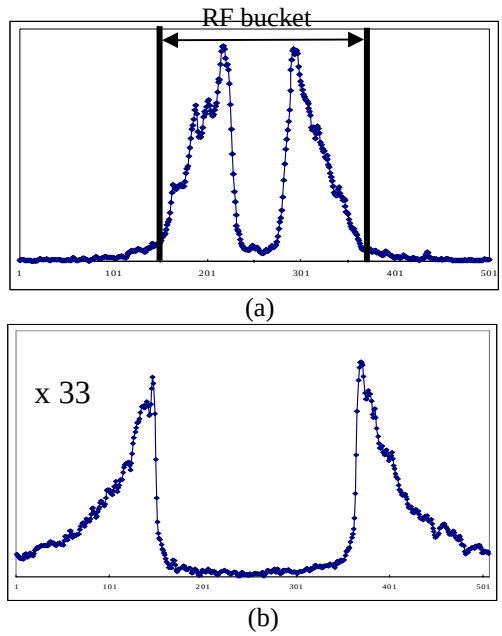

Figure 15: The projection of horizontal distributions of beam halos in Fig.14. (a) Strong beam halo. (b) Weak beam halo far outside.

From the lower picture of Fig. 15, the background level is 6 x 10^{-7} of the peak intensity. This background level is almost the same value as the estimated background from the Be-mirror as discussed in Section 5-2. We see two types of beam halo in Fig.15 (a). One is a strong halo having an intensity range of 10^{-4} in inside the area which corresponds to the separatrix of the RF bucket scaled by the value of the dispersion function at the source point. The other is a weak halo having an intensity range of 10^{-6} outside of this area.

CONCLUSION

We developed and constructed a coronagraph for the observation of the beam halo surrounding the beam. The optical polish of the objective lens is a key point in achieving a good S/N ratio, and we succeeded in obtaining a signal to background ratio 6x10^{-7}. To investigate the performance of the coronagraph, we measured the beam halo at the Photon Factory. As results, we observed a strong beam halo inside the RF bucket and a weak halo outside the RF bucket. The coronagraph is applicable not only to observing the beam halo, but also has many possibilities such as the observation of an injected beam under the presence of intense stored beam.

REFERENCE

[1] B.F.Lyot Month. Notice Roy. Ast. Soc, p580, **99** (1939.)